

Probing the Donor–Acceptor Proximity on the Physicochemical Properties of Porphyrin–Fullerene Dyads: “Tail-On” and “Tail-Off” Binding Approach

Francis D’Souza,^{*,†} Gollapalli R. Deviprasad,[†] Mohamed E. El-Khouly,[‡] Mamoru Fujitsuka,[‡] and Osamu Ito^{*,‡}

Contribution from the Department of Chemistry, Wichita State University, 1845 Fairmount, Wichita, Kansas 67260-0051, and Institute for Chemical Reaction Science, Tohoku University, Katahira, Sendai, 980-8577 Japan

Received February 8, 2001

Abstract: A new approach of probing proximity effects in porphyrin–fullerene dyads by using an axial ligand coordination controlled “tail-on” and “tail-off” binding mechanism is reported. In the newly synthesized porphyrin–fullerene dyads for this purpose, the donor–acceptor proximity is controlled either by temperature variation or by an axial ligand replacement method. In *o*-dichlorobenzene, 0.1 M (TBA)ClO₄, the synthesized zincporphyrin–fullerene dyads exhibit seven one-electron reversible redox reactions within the accessible potential window of the solvent and the measured electrochemical redox potentials and UV–visible absorption spectra reveal little or no ground-state interactions between the C₆₀ spheroid and porphyrin π -system. The proximity effects on the photoinduced charge separation and charge recombination are probed by both steady-state and time-resolved fluorescence techniques. It is observed that in the “tail-off” form the charge-separation efficiency changes to some extent in comparison with the results obtained for the “tail-on” form, suggesting the presence of some through-space interactions between the singlet excited zinc porphyrin and the C₆₀ moiety in the “tail-off” form. The charge separation rates and efficiencies are evaluated from the fluorescence lifetime studies. The charge separation via the singlet excited states of zinc porphyrin in the studied dyads is also confirmed by the quick rise–decay of the anion radical of the C₆₀ moiety within 20 ns. Furthermore, a long-lived ion pair with lifetime of about 1000 ns is also observed in the investigated zinc porphyrin–C₆₀ dyads.

Introduction

During the past decade, a significant amount research has been directed toward understanding the dynamics of photoinduced electron transfer in both protein and molecular systems due to their importance in photochemical conversion and storage of energy. As such, the natural and the artificial photosynthetic systems rely on spatially organized units with suitable photochemical and electrochemical properties.^{1,2} A number of covalently linked donor–acceptor dyads, triads, tetrads, etc., have been designed and studied for this purpose.² More recently, an increasing number of noncovalently linked, by means of metal–ligand coordinate bonds, hydrogen bonds, etc., donor–acceptor supramolecular assemblies have also been studied.³ Due to the

more biomimetic nature, the noncovalently linked self-assembled donor–acceptor systems are more appealing as model compounds.

Among the different donor–acceptor dyads, covalently linked porphyrin–quinone constitutes one of the most widely studied model compounds.² More recently, fullerenes⁴ C₆₀ and C₇₀ have been employed as electron acceptors^{5–8} due to their three-dimensional structure,⁹ reduction potentials comparable to benzoquinone,¹⁰ absorption spectrum extending most of the visible spectrum,¹¹ and small reorganization energy in electron-transfer reactions.¹² In the majority of the covalently linked donor–acceptor systems,^{5–8} the donor and acceptor entities are connected by a single bond. One of the problems of such model

[†] Wichita State University.

[‡] Tohoku University.

(1) (a) Disenhofer, J.; Michel, H. *Angew. Chem., Int. Ed. Engl.* **1989**, *28*, 829. (b) Feher, J. P.; Allen, M. Y.; Okamura, M. Y.; Rees, D. C. *Nature* **1989**, *339*, 111.

(2) (a) Maruyama, K.; Osuka, A. *Pure Appl. Chem.* **1990**, *62*, 1511. (b) Gust, D.; Moore, T. A. *Science* **1989**, *244*, 35. (c) Gust, D.; Moore, T. A. *Top. Curr. Chem.* **1991**, *159*, 103. (d) Gust, D.; Moore, T. A.; Moore, A. L. *Acc. Chem. Res.* **1993**, *26*, 198. (e) Wasielewski, M. R. *Chem. Rev.* **1992**, *92*, 435. (f) Paddon-Row, M. N. *Acc. Chem. Res.* **1994**, *27*, 18. (g) Sutin, N. *Acc. Chem. Res.* **1983**, *15*, 275. (h) Bard, A. J.; Fox, M. A. *Acc. Chem. Res.* **1995**, *28*, 141. (i) Meyer, T. J. *Acc. Chem. Res.* **1989**, *22*, 163. (j) Piotrowiak, P. *Chem. Soc. Rev.* **1999**, *28*, 143.

(3) (a) Ward, M. W. *Chem. Soc. Rev.* **1997**, *26*, 365 and references therein. (b) Hayashi, T.; Ogoshi, H. *Chem. Soc. Rev.* **1997**, *26*, 355. (c) Sessler, J. S.; Wang, B.; Springs, S. L.; Brown, C. T. In *Comprehensive Supramolecular Chemistry*; Atwood, J. L., Davies, J. E. D., MacNicol, D. D., Vögtle, F., Eds.; Pergamon: New York, 1996; Chapter 9.

(4) (a) Kroto, H. W.; Heath, J. R.; O’Brien, S. C.; Curl, R. F.; Smalley, R. E. *Nature* **1985**, *318*, 162. (b) Kratschmer, W.; Lamb, L. D.; Fostiropoulos, F.; Huffman, D. R. *Nature* **1990**, *347*, 345.

(5) (a) Khan, S. I.; Oliver, A. M.; Paddon-Row M. N.; Rubin, Y. *J. Am. Chem. Soc.* **1993**, *115*, 4919. (b) Saricifci, N. S.; Wudl, F.; Heeger, A. J.; Maggini, M.; Scorrano, G.; Prato, M.; Bourassa, J.; Ford, P. C. *Chem. Phys. Lett.* **1995**, *247*, 510. (c) Liddell, P. A.; Sumia, J. P.; Macpherson, A. N.; Noss, L.; Seely, G. R.; Clark, K. N.; Moore, A. L.; Moore, T. A.; Gust, D. *Photochem. Photobiol.* **1994**, *60*, 537. (d) Williams, R. M.; Zwier, J. M.; Verhoever, J. W. *J. Am. Chem. Soc.* **1995**, *117*, 4093. (e) Imahori, H.; Hagiwar, K.; Aoki, M.; Akiyama, T.; Taniguchi, S.; Okada, T.; Shirakawa, M.; Sakata, Y. *J. Am. Chem. Soc.* **1996**, *118*, 11771. (f) Kuciauskas, D.; Lin, S.; Seely, G. R.; Moore, A. L.; Moore, T. A.; Gust, D.; Drovetskaya, T.; Reed, C. A.; Boyd, P. D. W. *J. Phys. Chem.* **1996**, *100*, 15926. (g) Guldi, D. M.; Maggini, M.; Scorrano, G.; Prato, M. *J. Am. Chem. Soc.* **1997**, *119*, 974. (h) Imahori, H.; Yamada, K.; Hasegawa, M.; Taniguchi, S.; Okada, T.; Sakata, Y. *Angew. Chem., Int. Ed. Engl.* **1997**, *36*, 2626. (i) Liddell, P. A.; Kuciauska, D.; Sumida, J. P.; Nash, B.; Nguyen, D.; Moore, A. L.; Moore, T. A.; Gust, D. *J. Am. Chem. Soc.* **1997**, *119*, 1400.

compounds is the free rotation and flexibility of the single covalent bond which would give more than one conformer in solution. This eventually is expected to modulate the electronic interactions between the donor and acceptor entities, thus affecting the electron transfer rates. In porphyrin–quinone dyads, this problem has already been addressed by studying a few rigidly linked porphyrin–quinone dyads.¹³

In the present study, we have developed a novel approach to position the donor, zinc porphyrin, and acceptor, C₆₀, entities in defined spatial organization to probe the proximity effects. For this, covalently linked porphyrin–C₆₀ dyads capable of axial coordination of the functionalized C₆₀ entity via a “tail-on” and “tail-off” binding mechanism to the central zinc ion are developed (Scheme 1). The dyads, 2-(3'- or 4'-pyridyl)fulleropyrrolidine, covalently linked to one of the phenyl rings of a tetraphenylporphyrinatozinc macrocycle through the pyrrolidine ring nitrogen have newly been designed and synthesized. The donor–acceptor proximity on the efficiency of photoinduced electron transfer from the singlet excited zinc porphyrin to C₆₀ has been probed by controlling the axial coordination of the pyridyl group attached at the 2-position of the pyrrolidine ring of fulleropyrrolidine to the metal center of zinc porphyrin by two mechanisms, viz., (i) temperature-dependent axial coordination equilibrium and (ii) an intermolecular axial ligation controlled equilibrium using 3-picoline as shown in Scheme 1.

Results and Discussion

Synthesis of Porphyrin–Fullerene Conjugates. The synthetic procedure developed to probe the proximity effects in zinc porphyrin–C₆₀ dyads is shown in Scheme 2. This involves first synthesizing a α -amino acid appended porphyrin followed by condensing it with fullerene in the presence of a desired

pyridine aldehyde according to a general procedure developed by Maggini et al.¹⁴ for fulleropyrrolidine synthesis. The α -amino acid appended porphyrin was synthesized by first preparing 5-(3'-hydroxyphenyl)-10,15,20-triphenylporphyrin, **1a**, followed by converting it to 5-(3'-bromoethoxyphenyl)-10,15,20-triphenylporphyrin, **1b**.¹⁵ The 5-(3'-ethoxyphenyl-amino acetic acid)-10,15,20-triphenylporphyrin **1c** was obtained by treating **1b** with glycine methyl ester in methyl ethyl ketone containing excess potassium carbonate followed by hydrolysis of the ester in aqueous NaOH containing a THF solution. Free-base porphyrin–fullerene dyads **1d** and **2d** were metalated with zinc acetate¹⁶ to obtain the desired zinc porphyrin–fullerene conjugates **1** and **2**. Generally, good yields of the reaction products were obtained and the synthesized porphyrin–fullerene conjugates were found to be soluble in many organic solvents.

Electrochemical Studies. Cyclic voltammetric studies have been performed to evaluate the redox potentials and also to visualize any ground-state interactions between the porphyrin and fullerene entities in the studied porphyrin–fullerene conjugates. Figure 1 shows the cyclic voltammograms of **1** and **2** in 0.1 M (TBA)ClO₄, *o*-dichlorobenzene. Within the accessible potential window of the solvent, a total of seven reversible redox processes have been observed. The first and second redox potentials corresponding to the oxidation of the zinc porphyrin of **1** and **2** are virtually identical and are located at $E_{1/2} = 0.26$ and 0.61 V vs Fc/Fc⁺, respectively. The reduction potentials of the appended C₆₀ moiety of **1** are located at $E_{1/2} = -1.20$, -1.55 , and -2.07 V vs Fc/Fc⁺ and are not significantly different from that of **2**. Unlike the similarity between the oxidation potentials of the zinc porphyrin moieties of **1** and **2**, the corresponding potentials for the porphyrin ring reduction reveal small changes. That is, the potentials for the zinc porphyrin ring reduction of **1** are located at $E_{1/2} = -1.97$ and -2.36 V vs Fc/Fc⁺, respectively, and are 20–40 mV negatively shifted compared to the corresponding porphyrin ring reduction potentials of **2**. However, these potentials are not significantly different from that earlier reported for tetraphenylporphyrinatozinc, ZnTPP, and fulleropyrrolidines.^{7a,17} These results collectively suggest weak or no ground-state interactions between the zinc porphyrin and C₆₀ entities.

Addition of 3-picoline to a solution of **1** or **2**, that is, to produce the “tail-off” form according to Scheme 1b while keeping the coordination number of the central zinc the same, revealed no significant changes in the redox potentials. This suggests that replacing the coordinated pyridine of the fulleropyrrolidine unit by externally added 3-picoline does not change the electronic structure of the porphyrin π -system to an appreciable extent.

Temperature-Dependent “Tail-On” and “Tail-Off” Binding. The optical absorption spectrum of the zinc porphyrin–

(6) (a) Dietel, E.; Hirsh, A.; Eichhorn, E.; Rieker, A.; Hackbarth, S.; Roder, B. *Chem. Commun.* **1998**, 1981. (b) Gareis, T.; Kothe, O.; Daub, J. *Eur. J. Org. Chem.* **1998**, 1549. (c) Da Ros, T.; Prato, M.; Guldi, D.; Alessio, E.; Ruzzi, M.; Pasimeni, L.; Carano, M.; Paolucci, F.; Ceroni, P.; Roffia, S. In *Recent Advances in the Chemistry and Physics of Fullerenes and Related Materials*; Kadish, K. M., Ruoff, R. S., Eds.; The Electrochemical Proceedings Series, Pennington, NJ, 1998; p 1074. (d) Martin, N.; Sanchez, L.; Illescas, B.; Perez, I. *Chem. Rev.* **1998**, *98*, 2527. (e) Gareis, T.; Kothe, O.; Daub, J. *Eur. J. Org. Chem.* **1998**, 1549. (f) Martin, N.; Sanchez, L.; Illescas, B.; Perez, I. *Chem. Rev.* **1998**, *98*, 2527.

(7) (a) D'Souza, F.; Deviprasad, G. R.; Rahman, M. S.; Choi, J.-P. *Inorg. Chem.* **1999**, *38*, 2157. (b) Armaroli, N.; Diederich, F.; Echegoyen, L.; Habicher, T.; Flamigni, L.; Marconi, G.; Nierengarten, J.-F. *New J. Chem.* **1999**, *77*. (c) Da Ros, T.; Prato, M.; Guldi, D. M.; Alessio, E.; Ruzzi, M.; Pasimeni, L. *Chem. Commun.* **1999**, 635. (d) Tashiro, K.; Aida, T.; Zheng, J.-Y.; Kinbara, K.; Saigo, K.; Sakamoto, S.; Yamaguchi, K. *J. Am. Chem. Soc.* **1999**, *121*, 9477. (e) Tkachenko, N. V.; Rantala, L.; Tauber, A. Y.; Helaja, J.; Hynninen, P. H.; Lemmetyinen, H. *J. Am. Chem. Soc.* **1999**, *121*, 9378.

(8) (a) Guldi, D. M. *Chem. Commun.* **2000**, 321. (b) Armaroli, N.; Marconi, G.; Echegoyen, L.; Bourgeois, J.-P.; Diederich, F. *Chem. Eur. J.* **2000**, *6*, 1629. (c) Guldi, D. M.; Luo, C.; Da Ros, T.; Prato, M.; Dietel, E.; Hirsch, A.; *Chem. Commun.* **2000**, 375. (d) Luo, C.; Guldi, D. M.; Imahori, H.; Tamaki, K.; Sakata, Y. *J. Am. Chem. Soc.* **2000**, *122*, 6535. (e) Kuciauskas, D.; Liddell, P. A.; Lin, S.; Stone, S. G.; Moore, A. L.; Moore, T. A.; Gust, D. *J. Phys. Chem. B.* **2000**, *104*, 4307. (f) Schuster, D. I.; Cheng, P.; Wilson, S. R.; Prokhorenko, V.; Katterle, M.; Holzwarth, A. R.; Braslavsky, S. E.; Klihm, G.; Williams, R. M. Luo, C. *J. Am. Chem. Soc.* **2000**, *121*, 11599. (g) Imahori, H.; El-Khouly, M. E.; Fujitsuka, M.; Ito, O.; Sakata, Y.; Fukuzumi, S. *J. Phys. Chem. A.* **2001**, *105*, 325.

(9) *Fullerene and Related Structures*; Hirsch, A., Ed.; Springer: Berlin, 1999; Vol. 199.

(10) (a) Allemann, P. M.; Koch, A.; Wudl, F.; Rubin, Y.; Diederich, F.; Alvarez, M. M.; Anz, S. J.; Whetten, R. L. *J. Am. Chem. Soc.* **1991**, *113*, 1050. (b) Xie, Q.; Perez-Cordero, E.; Echegoyen, L. *J. Am. Chem. Soc.* **1992**, *114*, 3978.

(11) Ajie, H.; Alvarez, M. M.; Anz, S. J.; Beck, R. E.; Diederich, F.; Fostiropoulos, K.; Huffman, D. R.; Kratschmer, W.; Rubin, Y.; Schriver, K. E.; Sensharma, E.; Whetten, R. L. *J. Phys. Chem.* **1990**, *94*, 8630.

(12) Imahori, H.; Hagiwara, K.; Akiyama, T.; Aoki, M.; Taniguchi, S.; Okada, T.; Shirakawa, M.; Sakata, Y. *Chem. Phys. Lett.* **1996**, *263*, 545.

(13) (a) Connolly, J. S.; Bolton, J. R. In *Photoinduced Electron Transfer*; Fox, M. A., Channon, M., Eds.; Elsevier: Amsterdam, 1988; Part D, pp 303–393. (b) Antolovich, M.; Keyte, P. J.; Oliver, A. M.; Paddon-Row, M. N.; Droon, J.; Verhoever, J. W.; Jonker, S. A.; Warman, J. M. *J. Phys. Chem.* **1991**, *95*, 1933. (c) Macpherson, A. N.; Liddell, P. A.; Lin, S.; Noss, L.; Seely, G. R.; DeGraziano, J. M.; Moore, A. L.; Moore, T. A.; Gust, D. *J. Am. Chem. Soc.* **1995**, *117*, 7202.

(14) (a) Maggini, M.; Scorrano, G.; Prato, M. *J. Am. Chem. Soc.* **1993**, *115*, 9798. (b) Prato, M.; Maggini, M.; Giacometti, C.; Scorrano, G.; Sandona, G.; Farnia, G. *Tetrahedron*, **1996**, *52*, 5221.

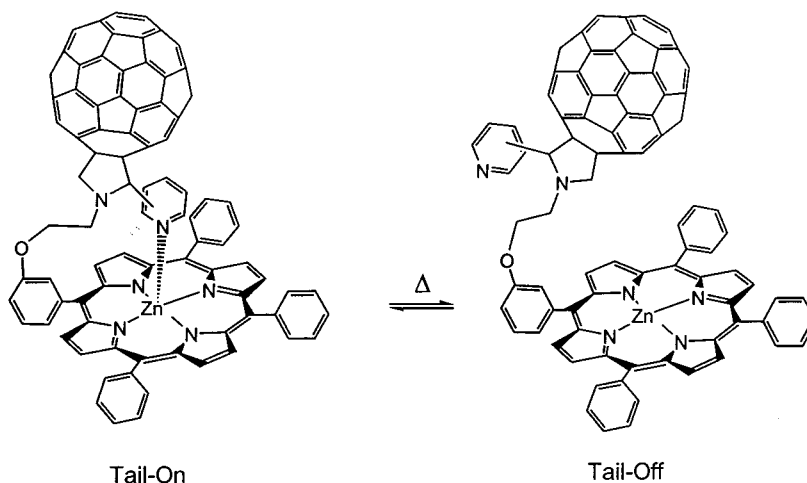
(15) D'Souza, F.; Krishnan, V. *Inorg. Chim. Acta* **1990**, *176*, 131.

(16) Smith, K. M. *Porphyrins and Metalloporphyrins*; Elsevier: New York, 1977.

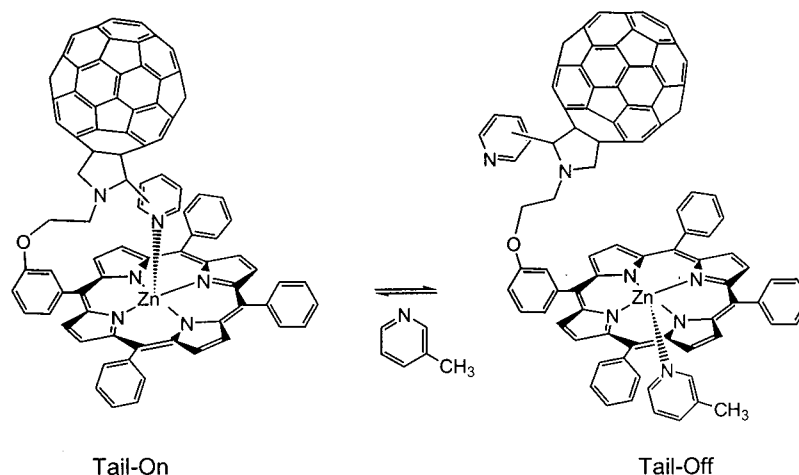
(17) (a) Deviprasad, G. R.; Zandler, M. E.; D'Souza, F. In *Fullerenes 2000: Electrochemistry and Photochemistry*; Fukuzumi, S., D'Souza, F., Guldi, D. M., Eds.; *Proc. Electrochem. Soc.* **2000**, *8*, 182. (b) Kutner, W.; Noworyta, K.; Deviprasad, G. R.; D'Souza, F. *J. Electrochem. Soc.* **2000**, *147*, 2647.

Scheme 1

(a) Temperature Dependent Equilibrium



(b) Axial Ligand Controlled Equilibrium



fullerene conjugates revealed absorption bands characteristic of both zinc porphyrin and fullerene entities. At room temperature, the Soret bands of **1** and **2** are located at around 433 nm, and this compares with a 425 nm Soret band of ZnTPP and 434 nm band of pentacoordinated ZnTPP–pyridine complex. These results suggest the existence of a pentacoordinated zinc porphyrin due to the axial coordination of the pyridyl unit of the fulleropyrrolidine entity, a result similar to that reported by us earlier for a pyridine-appended zinc porphyrin complex.¹⁸ Concentration dependence studies revealed no changes in the peak maxima, indicating the absence of any intermolecular-type interactions.

Interestingly, temperature dependence studies reveal the occurrence of “tail-on” and “tail-off” type binding as shown in Scheme 1a in the studied compounds. Figure 2 shows the resulting spectral changes and the figure inset shows a Van’t Hoff plot of $-\ln K$ vs T^{-1} . The binding constants obtained by the Scatchard method¹⁹ and the calculated thermodynamic

parameters are given in Table 1. An examination of Table 1 reveals that the binding constants are 5–6 times larger for the investigated compounds than those in the earlier reported pyridine appended zinc porphyrin¹⁸ and the majority of the equilibrium is in the “tail-on” form. Between compounds **2** and **1**, compound **2**, the *m*-pyridyl derivative, revealed a higher binding constant. The values of the thermodynamic parameter suggest that the higher K value is a result of both entropy and enthalpy contributions.

Axial Ligand Controlled “Tail-On” and “Tail-Off” Binding. To probe the effect of “tail-on” and “tail-off” forms of the dyads on the efficiencies of photoinduced electron transfer from singlet excited zinc porphyrin to fullerene, we have utilized an axial ligand replacement method (Scheme 1b) to obtain the “tail-off” form instead of the temperature variation approach to avoid any temperature variation induced changes in the fluorescence quantum yields. The progress of the reaction shown in Scheme 1b was monitored by ¹H NMR studies (data not shown). The

(18) D’Souza, F.; Hsieh, Y.-Y.; Deviprasad, G. R. *Inorg. Chem.* **1996**, *35*, 5747.

(19) Scatchard, G. *Ann. N.Y. Acad. Sci.* **1949**, *51*, 661.

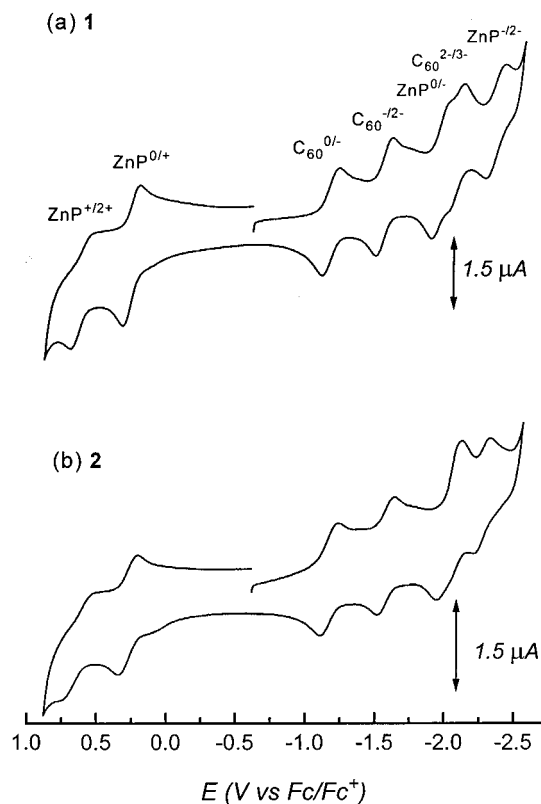


Figure 1. Cyclic voltammograms of **1** and **2** in 0.1 M (TBA)ClO₄, *o*-dichlorobenzene. Scan rate = 100 mV/s. Note the overlapping C₆₀²⁻³⁻ and ZnP^{0/-} redox processes for **2**.

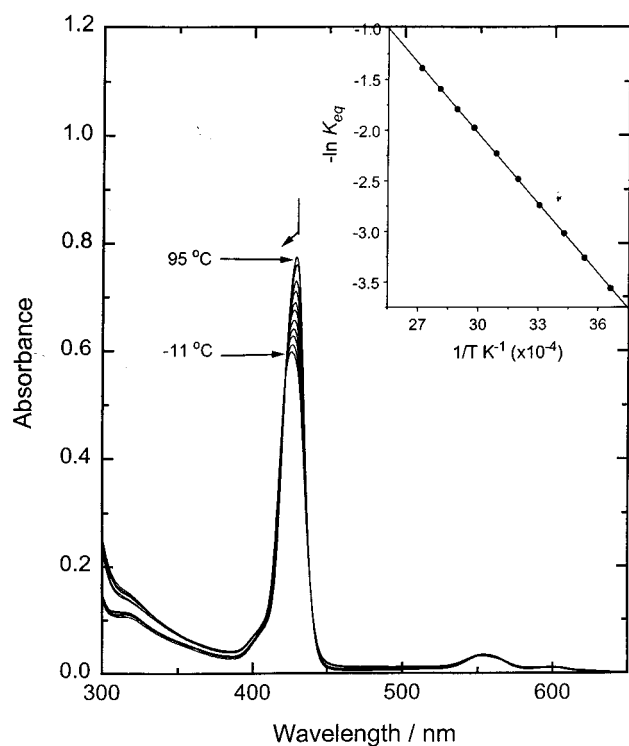


Figure 2. UV–visible spectral changes observed for **2** as a function of temperature in *o*-dichlorobenzene. The inset figure shows Van't Hoff plot of $-\ln K$ vs T^{-1} .

of the complexed fulleropyrrolidine unit. Energy minimization calculations^{17a,21} and CPK model building studies revealed an

(20) D'Souza, F.; Rath, N. P.; Deviprasad, G. R.; Zandler, M. E. *Chem. Commun.* **2001**, 267.

Table 1. Equilibrium Constant, K_a , as Well as the Thermodynamic Parameters for the Temperature-Controlled “Tail-On” and “Tail-Off” Processes of Zinc Porphyrin–C₆₀ Dyads in *o*-Dichlorobenzene

dyad	K_a , ^a M ⁻¹	ΔG , kJ mol ⁻¹	ΔH , kJ mol ⁻¹	ΔS , J K ⁻¹ mol ⁻¹
2	17.29	-7.07	-19.17	-40.59
1	14.43	-6.62	-18.11	-38.52
ZnP _m ~py ^b	2.99	-2.72	-45.36	-138.6

^a At 298.15 K. ^b From ref 18; py = pyridine.

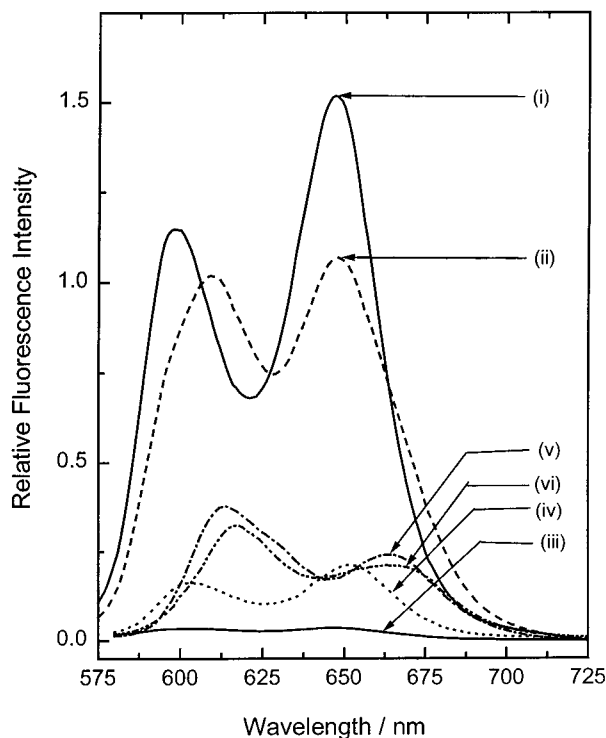


Figure 3. Room-temperature steady-state fluorescence spectrum of (i) ZnTPP, (ii) ZnTPP + picoline (10 equiv), (iii) **2**, (iv) **1**, (v) **2** + picoline (10 equiv), and (vi) **1** + picoline (10 equiv) in *o*-dichlorobenzene. The concentration of porphyrins was maintained at 2 μ M. λ_{ex} = 555 nm.

almost similar distance of ~ 9.5 Å between the porphyrin center to the C₆₀ center in the “tail-on” mode. In the “tail-off” form, this distance varied between 11 and 13 Å depending up on the different orientations of the fulleropyrrolidine group with respect to the zinc porphyrin, suggesting that the different donor–acceptor distances between the “tail-on” and “tail-off” forms may be responsible for the fluorescence intensity variations. In addition, effect ii, that is, the minor structural changes, may also contribute to the emission changes. To verify these, picosecond time-resolved emission studies have been performed.

Picosecond Time-Resolved Fluorescence Spectra. The overall time-resolved fluorescence spectral results are essentially same as those observed from steady-state measurements. The decay time profiles for **1** and **2** along with ZnTPP in the presence and absence of added 3-picoline are shown in Figure 4. The evaluated fluorescence lifetimes are summarized in Table 2, in which the charge separation rates and quantum yields, evaluated in the usual manner,^{8g} are also listed. A monoexponential decay for ZnTPP in *o*-dichlorobenzene is observed both in the presence and absence of added 3-picoline. The calculated lifetime for ZnTPP is found to be 10–20% smaller for the

(21) D'Souza, F.; Zandler, M. E.; Deviprasad, G. R.; Kutner, W. J. *Phys. Chem. A* **2000**, 104, 6887.

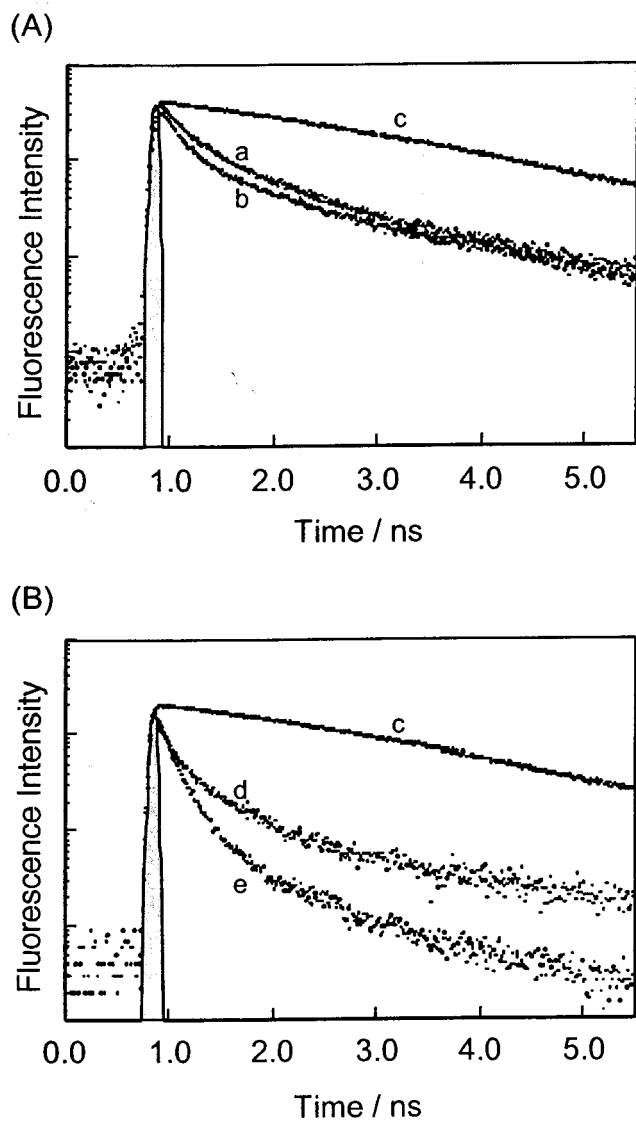


Figure 4. Fluorescence decay profiles (A and B) of (a) **2**, (b) **2** + picoline (10 equiv), (c) ZnTPP, (d) **1**, and (e) **1** + picoline (10 equiv) in *o*-dichlorobenzene. $\lambda_{\text{ex}} = 555$ nm.

pentacoordinated ZnTPP–picoline complex. This suggests the occurrence of excited-state reactions most probably involving the coordinated picoline acting as an electron donor to the singlet excited porphyrin.²²

Interestingly, the calculated lifetimes of the dyads, both in the “tail-on” and “tail-off” forms, are found to be much smaller than that of the pristine ZnTPP and the ZnTPP–picoline complex, indicating the occurrence of efficient charge separation from the singlet excited state of the zinc porphyrin both in the “tail-on” and “tail-off” forms. The emission decay of **1** and **2** follows a biexponential decay both in the presence and absence of 3-picoline probably due to the existence of an equilibrium process involving the “tail-on” and “tail-off” forms as well as one or more conformers of each of these two forms in solution.

In contrast to the results of steady-state emission where an increase in the intensity is observed in the “tail-off” form of the dyads, the time-resolved emission studies reveal different trends. That is, the measured lifetimes reveal a decrease in the overall lifetimes (both short and long components of the biexponential decay) on addition of picoline. This suggests that the release of the intramolecularly coordinated pyridine moiety

facilitates conformational changes favorable for through-space charge separation. In addition, the coordinated 3-picoline in the “tail-off” state might also cause additional quenching acting as an electron donor, like that observed in the case of the ZnTPP–picoline complex. Between **1** and **2**, rates of charge separation, k_{cs} , and quantum yield, Φ_{cs} , did not show any specific trend. In the case of **1**, the k_{cs} and Φ_{cs} increase slightly in the “tail-off” form, while reverse trend is observed for **2**. Although the magnitude of these changes is relatively small, these results suggest that the “tail-on” form of **1** accelerates the charge separation, a trend similar to that seen from the steady-state measurements. However, the different magnitudes of quenching between the steady-state and time-resolved emission studies suggest that in addition to the charge-separation quenching the minor structural changes might also induce quenching (static) of the excited porphyrin in the steady-state emission.

Nanosecond Transient Absorption Spectra. Transient absorption spectra for **1** and **2** in the presence and absence of 3-picoline in *o*-dichlorobenzene are shown in Figures 5 and 6, in which the 700 nm band was attributed to the triplet state of the C₆₀ moiety.²³ The 850 nm band was attributed to the triplet state of the zinc porphyrin moiety.²³ The 1000 nm band was attributed to the radical anion of the C₆₀ moiety.²⁴ The transient absorption bands due to the triplet state decay smoothly with lifetimes of 600 ns. The time profile of the radical anion of the C₆₀ moiety shows two components: one is quick rise–decay and another is slower decay similar to those of the triplet states. The absorbance ratio at 1000 nm to that at 700 nm for **1** in the presence of 3-picoline is 0.6 (= 0.08/0.13 from the spectrum at 100 ns in Figure 5b), which is large enough to assign the slow decay part of the 1000 nm band to the anion radical of C₆₀. Thus, there are two types of decays in the charge-separated states: one is fast decay and the other is slow decay.

This behavior of fast and slow decay could be due to the following: (i) Generation of a second charge-separated state from a triplet state formed through a quick charge recombination. The ion pair produced via the second charge separation has the triplet state character, which shows a longer lifetime than the ion pair with the singlet state character. (ii) The first charge recombination occurs in three ways: the first part is to the ground state, the second part is to the triplet excited state, and third part remains as the long-lived ion pair, which is in equilibrium with the triplet state. From the comparison with the time profile at 700 nm, which is similar to the decay rate of the slower part at 1000 nm, this interpretation seems feasible in these dyads.

The quick rise–decay suggests that electron transfer from the singlet excited zinc porphyrin to the C₆₀ entity occurs. The fluorescence lifetime supports such a fast charge separation. As explained before, the slow decay component of the ion pair may be ascribed to long-lived ion pair, because the absorption peak at 1000 nm is observed in the spectra at 0.1 and 1.0 μs time intervals. On addition of 3-picoline, the 1000 nm band with quick rise–decay appears (Figure 5), indicating that the charge separation takes place in the “tail-off” form. The relative absorption intensity of **1** at 1000 to 700 nm in the presence of 3-picoline (0.6 at 100 ns) is slightly larger than that in the absence of 3-picoline (0.025/0.06 = 0.42 at 100 ns from Figure 5a). This implies that the charge separation in the “tail-off” is as efficient as “tail-on”, which is in good agreement with the conclusion from the time-resolved emission studies.

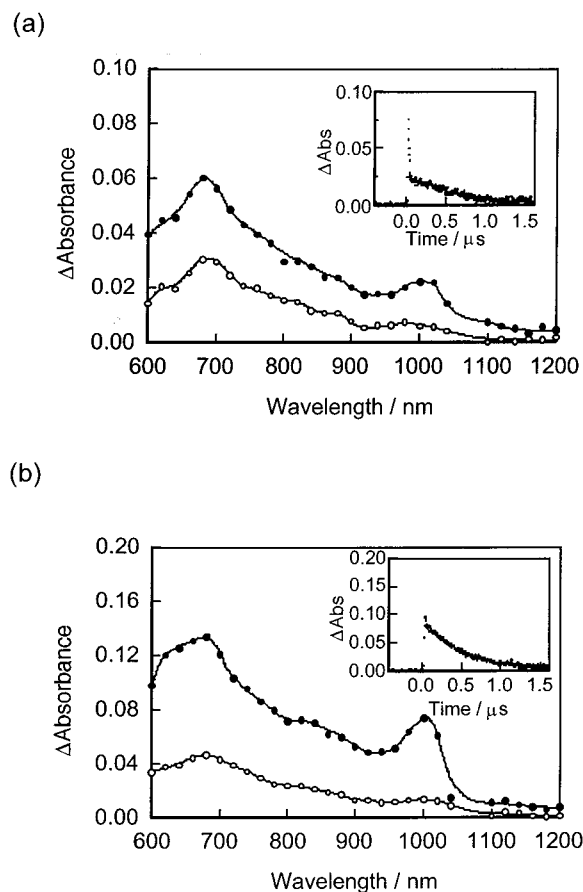
(23) Nojiri, T.; Watanabe, A.; Ito, O. *J. Phys. Chem. A* **1998**, *102*, 5215.

(24) Fujitsuka, M.; Ito, O.; Yamashiro, T.; Aso, Y.; Otsubo, T. *J. Phys. Chem. A* **2000**, *104*, 4876.

(22) Barbooy, N.; Feitelson, J. *J. Phys. Chem.* **1984**, *88*, 1065.

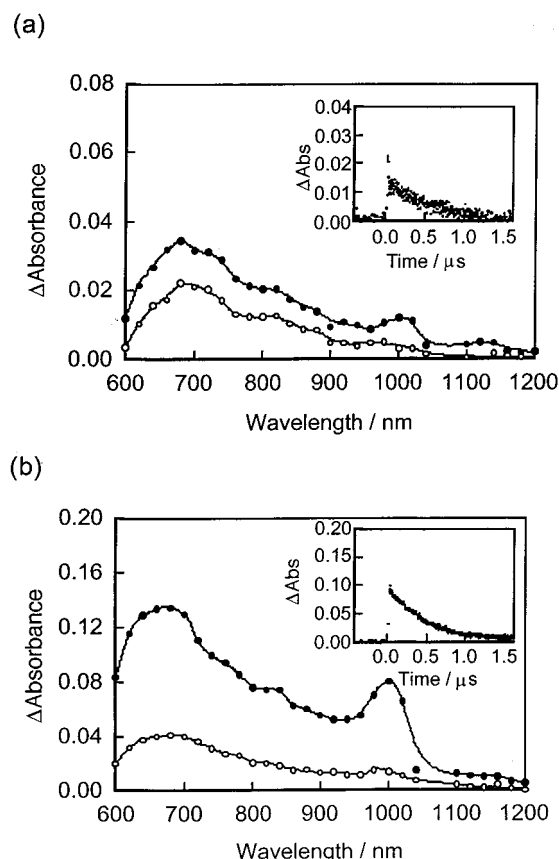
Table 2. Fluorescence Lifetimes (τ_f), Charge-Separation Rate Constants (k_{cs}), Charge-Separation Quantum Yields (Φ_{cs}), Fast Charge-Recombination Rate Constants (k_{cr}^f), and Slow Charge-Recombination Rate Constants (k_{cr}^s) of the Investigated Zinc Porphyrin–C₆₀ Dyads in *o*-Dichlorobenzene in the Absence and Presence of 3-Picoline

compound	τ_f /ps (%)		k_{cs}/s^{-1}	Φ_{cs}	k_{cr}^f/s^{-1}^a	k_{cr}^s/s^{-1}
ZnTPP	2030					
ZnTPP + picoline (10 equiv)	1740					
ZnTPP + picoline (200 equiv)	1620					
1	284 (87%)	1950 (13%)	5.1×10^9	0.93	(5×10^7)	1.3×10^6
1 + picoline (10 equiv)	197 (93%)	1490 (7%)	4.7×10^9	0.92	(5×10^7)	1.6×10^6
1 + picoline (200 equiv)	177 (96%)	1470 (4%)				
2	321 (76%)	1660 (24%)	3.0×10^9	0.89	(5×10^7)	0.9×10^6
2 + picoline (10 equiv)	221 (82%)	1510 (18%)	5.2×10^9	0.93	(5×10^7)	1.9×10^6
2 + picoline (200 equiv)	177 (96%)	1470 (4%)				

^a Values at first approximation.**Figure 5.** Transient absorption spectra obtained by the 530 nm nanosecond laser photolysis of (a) **1** (0.05 mM) and (b) **1** + picoline (10 equiv) in *o*-dichlorobenzene; filled circle is spectrum at 100 ns and open circle at 1000 ns. Inset: time profile at 1000 nm.

For **2**, similar transient absorption spectra were obtained (Figure 6), which indicates that the charge separation via the singlet excited state takes place in both the “tail-on” and “tail-off” forms. The efficiency of the charge separation is also slightly higher for the “tail-off” form.

Summary. We have successfully demonstrated a new approach of probing proximity effects in porphyrin–fullerene based donor–acceptor dyads by using a “tail-on” and “tail-off” binding mechanism. The cyclic voltammetric and optical absorption spectral studies revealed no significant ground-state interactions between the porphyrin π -ring and the C₆₀ spheroid. The results of steady-state and time-resolved fluorescence emission reveal that in the “tail-off” form the charge-separation rates and efficiency change slightly in comparison with the results of the “tail-on” form, suggesting the presence of some

**Figure 6.** Transient absorption spectra obtained by the 530 nm nanosecond laser photolysis of (a) **2** (0.05 mM) and (b) **2** + picoline (10 equiv) in *o*-dichlorobenzene; filled circle is spectrum at 100 ns and open circle at 1000 ns. Inset: time profile at 1000 nm.

through-space interactions between the singlet excited zinc porphyrin and C₆₀ moiety in the “tail-off” form. In the studied dyads, the charge separation via the singlet excited states of zinc porphyrin is also confirmed by the quick rise–decay of the anion radical of the C₆₀ entity within 20 ns. Furthermore, a long-lived ion pair with a lifetime of about 1000 ns is also observed in these systems.

Experimental Section

Chemicals. Buckminsterfullerene, C₆₀ (+99.95%), was from Bucky-USA (Bellaire, TX). *o*-Dichlorobenzene in a sure seal bottle, methyl glycine ester hydrochloride, pyridine carboxaldehydes, pyrrole, benzaldehyde, 3-hydroxybenzaldehyde, and tetra-*n*-butylammonium perchlorate, (TBA)ClO₄, were from Aldrich Chemicals (Milwaukee, WI). All chemicals were used as received. Solvents used in the present study are all the purest grade commercially available. The newly

synthesized compounds were freshly purified by column chromatography, and their purity was tested by TLC prior to spectral measurements.

Synthesis of 5-(3'-Hydroxyphenyl)-10,15,20-triphenylporphyrin, 1a. Compound **1a** was synthesized by reacting 3-hydroxybenzaldehyde (1.5 g, 12 mM), benzaldehyde (3.9 g, 37 mM), and pyrrole (3.3 g, 49 mM) in refluxing propionic acid. The crude product was purified on a basic alumina column with chloroform/methanol (95:5 v/v) as eluent. Yield 10%. ¹H NMR in CDCl₃, δ ppm: 8.76 (m, 8H, β-pyrrole), 8.16 (m, 6H, *o*-phenyl), 7.71 (m, 9H, *o*-*p*-phenyl), 7.96–7.12 (d, t, t, d, 4H, substituted phenyl), 5.87 (s, br, 1H, hydroxy), –2.76 (s, br, 2H, imino).

Synthesis of 5-(3'-Bromoethoxyphenyl)-10,15,20-triphenylporphyrin, 1b. This was synthesized by reacting **1a** (0.1 g, 0.16 mM) and an excess of 1,2-dibromoethane in DMF containing potassium carbonate for 24 h.¹⁴ Crude **1b** was purified on basic alumina with chloroform/hexane (90:10 v/v) as the eluent. Yield 87%. ¹H NMR: 8.82 (m, 8H, β-pyrrole), 8.18 (m, 6H, *o*-phenyl), 7.73 (m, 9H, *m*-*p*-phenyl), 7.83–7.28 (d, t, d, 4H, substituted phenyl), 4.45 (t, 2H, –CH₂–), 3.70 (t, 2H, –CH₂–), –2.85 (s, br, 2H, imino).

Synthesis of 5-(3'-Ethoxyphenyl-amino acetic acid)-10,15,20-triphenylporphyrin 1c. For this, first the methyl ester of **1c** was synthesized by reacting **1b** (0.5 g, 0.7 mM) and glycine methyl ester (0.6 g, 7 mM) in methyl ethyl ketone containing excess potassium carbonate. The crude product was purified on a silica gel column with chloroform. ¹H NMR: 8.86 (m, 8H, β-pyrrole), 8.19 (m, 6H, *o*-phenyl), 7.76 (m, 9H, *m*-*p*-phenyl), 7.86–7.18 (d, t, d, 4H, substituted phenyl), 4.86 (s, 2H, –CH₂–), 4.52 (t, 2H, –CH₂–), 3.92 (t, 2H, –CH₂–), 3.14 (s, 3H, CH₃), –2.89 (s, br, 2H, imino). **1c** was synthesized by refluxing the methyl ester in THF:water (95:5 v/v) with a few drops of 50% aqueous NaOH. Crude **1c** was purified on a silica gel column with chloroform:methanol (80:20 v/v). Yield 70%.

Synthesis of 5-(3'-Phenoxyethyl-N-(2-(3'-pyridyl)fulleropyrroline))-10,15,20-triphenylporphyrin, 2d. To compound **1c** (0.06 g, 0.08 mM) in toluene were added 3-pyridine carboxaldehyde (0.044 g, 0.4 mM) and C₆₀ (0.295 g, 0.4 mM), and the solution was refluxed for 12 h. The crude product was purified on a silica gel column with toluene:ethyl acetate (90:10 v/v). Yield 28%. ¹H NMR: 8.99 (d, 1H, *o*-pyridyl), 8.82 (m, 8H, β-pyrrole), 8.19 (m, 6H, *o*-phenyl), 8.55 (d, 1H, *o*-pyridyl), 8.08 (d, 1H, *p*-pyridyl), 7.72 (m, 9H, *m*-*p*-phenyl), 7.33 (q, 1H, *m*-pyridyl), 8.03–7.17 (d, t, d, 4H, substituted phenyl), 6.57–5.62 (d, s, d, 3H, pyrrolidine) 4.52 (t, 2H, –CH₂–), 4.02 (t, 2H, –CH₂–), –2.91 (s, br, 2H, imino).

Synthesis of 5-(3'-Phenoxyethyl-N-(2-(4'-pyridyl)fulleropyrroline))-10,15,20-triphenylporphyrin, 1d. To compound **1c** (0.06 g, 0.08 mM) in toluene were added 4-pyridine carboxaldehyde (0.044 g, 0.4 mM) and C₆₀ (0.295 g, 0.4 mM), and the solution was refluxed for 12 h. The crude product was purified on a silica gel column with toluene:ethyl acetate (90:10 v/v). Yield 25%. ¹H NMR: 8.93 (m, 8H, β-pyrrole), 8.66 (d, 2H, *o*-pyridyl), 8.23 (m, 6H, *o*-phenyl), 7.73 (d, 2H, *p*-pyridyl), 7.78 (m, 9H, *m*-*p*-phenyl), 8.03–7.17 (d, t, d, 4H, substituted phenyl), 5.07–4.07 (d, s, d, 3H, pyrrolidine) 4.52 (t, 2H, –CH₂–), 4.02 (t, 2H, –CH₂–), –2.91 (s, br, 2H, imino-H).

Synthesis of 5-(3'-Phenoxyethyl-N-(2-(3'-pyridyl)fulleropyrroline))-10,15,20-triphenylporphyrinatozinc(II), 2. Compound **2** was synthesized by metalation of **2d** with zinc acetate.¹⁵ To a solution of **2d** (0.2 g, 0.15 mM) in CHCl₃ was added excess zinc acetate in

methanol. This solution was stirred for 30 min. The solvent was removed under reduced pressure, and the crude product was dissolved in CH₂Cl₂, washed with water, and dried with sodium sulfate. The solution was concentrated and loaded on to a basic alumina column. Pure **2** was eluted with chloroform:hexane (90:10 v/v). Yield 94%. ¹H NMR: 8.81 (m, 8H, β-pyrrole), 8.19 (m, 6H, *o*-phenyl), 7.64 (m, 9H, *m*-*p*-phenyl), 8.03–6.72 (d, t, d, 4H, substituted phenyl), 6.78 (d br, 1H, *p*-pyridyl), 4.83 (s br, 1H, *m*-pyridyl), 4.87–4.26 (s br, s br, s br, 3H, pyrrolidine) 3.84 (s br, 4H, –CH₂–), 3.68 (d br, 2H, *o*-pyridyl). ESI mass in CH₂Cl₂, calcd 1558.3, found 1559.4.

Synthesis of 5-(3'-Phenoxyethyl-N-(2-(4'-pyridyl)fulleropyrroline))-10,15,20-triphenylporphyrinatozinc(II), 1. This was synthesized by metalation of **1d** with zinc acetate. To a solution of **1d** (0.2 g, 0.3 mM) in CHCl₃ was added excess zinc acetate in methanol. This solution was stirred for 30 min. The solvent was removed under reduced pressure, and the crude product was dissolved in CH₂Cl₂, washed with water, and dried with sodium sulfate. The solution was concentrated and loaded onto a basic alumina column. Pure **1** was eluted with chloroform:hexane (90:10 v/v). Yield 94%. ¹H NMR: 8.83 (m, 8H, β-pyrrole), 8.19 (m, 6H, *o*-phenyl), 7.65 (m, 9H, *m*-*p*-phenyl), 8.05–6.63 (d, t, d, 4H, substituted phenyl), 6.48 (d br, 2H, *p*-pyridyl), 4.87–4.26 (s br, s br, s br, 3H, pyrrolidine), 3.84 (s br, 4H, –CH₂–), 3.42 (d br, 2H, *o*-pyridyl). ESI mass in CH₂Cl₂, calcd 1558.3, found 1559.5.

Instrumentation. The UV–visible spectral measurements were carried out with a Shimadzu model 1600 UV–visible spectrophotometer. The fluorescence was monitored by using a Spex Fluorolog spectrometer. A right angle detection method was used. The ¹H NMR studies were carried out on a Varian 400 MHz spectrometer. Tetramethylsilane (TMS) was used as an internal standard. Cyclic voltammograms were obtained by using a conventional three-electrode system on an EG&G model 263A potentiostat/galvanostat. A platinum or a glassy carbon disk electrode was used as the working electrode. A platinum wire was served as the counterelectrode. An Ag/AgCl electrode, separated from the test solution by a fritted supporting electrolyte/solvent bridge, was used as the reference electrode. The potentials were referenced to an internal ferrocene/ferrocenium redox couple. All the solutions were purged prior to spectral and electrochemical measurements using argon gas.

Nanosecond transient absorption spectra in the NIR region were measured by means of laser flash photolysis; 532 nm light from a Nd:YAG laser was used as the exciting source and a Ge-avalanche-photodiode module was used for detecting the monitoring light from a pulsed Xe lamp as described in our previous report.²⁵ The picosecond time-resolved fluorescence spectra were measured using an argon-ion pumped Ti:sapphire laser (Tsunami) and a streak scope (Hamamatsu Photonics). The details of the experimental setup are described elsewhere.²⁵

Acknowledgment. The authors thank the donors of the Petroleum Research Fund, administered by the American Chemical Society, for support of this work.

JA010356Q

(25) (a) Matsumoto, K.; Fujitsuka, M.; Sato, T.; Onodera, S.; Ito, O. *J. Phys. Chem. B* **2000**, *104*, 11632. (b) Komamine, S.; Fujitsuka, M.; Ito, O.; Morikawa, K.; Miyata, T.; Ohno, T. *J. Phys. Chem. A* **2000**, *104*, 11497.